Electronic Supplementary Information

BSA-templated MnO_2 nanoparticles as both peroxidase and oxidase mimics

Xing Liu,[a] Qi Wang,[a] Huihui Zhao,[a] Lichun Zhang,[a] Yingying Su[b] and Yi Lv[a*]

[a] College of Chemistry, Sichuan University, Chengdu, Sichuan 610064, China.

[b] Analytical & Testing Center, Sichuan University, Chengdu, Sichuan 610064, China.

[*]Corresponding author. Fax/Tel.: +86 02885412798

E-mail address: lvy@scu.edu.cn

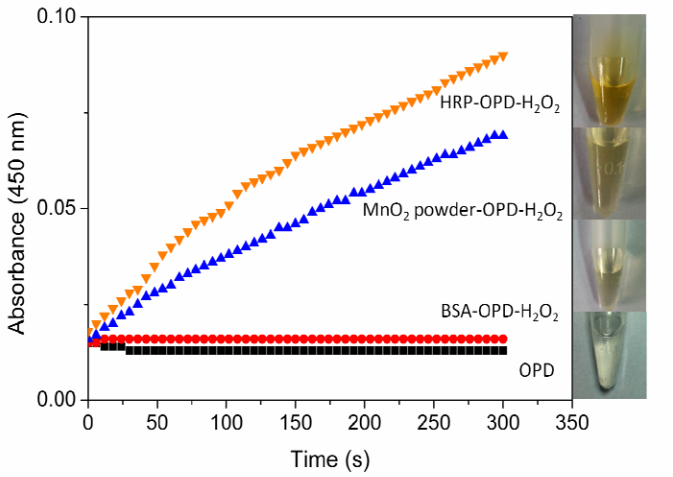

Fig. S1. The time-dependent absorbance changes at 450 nm of OPD in the presence of H_2O_2 with 3.3 μg mL^{-1} HRP or 3.7 μg mL^{-1} micrometer sized MnO_2 powder or 3.7 μg mL^{-1} BSA.

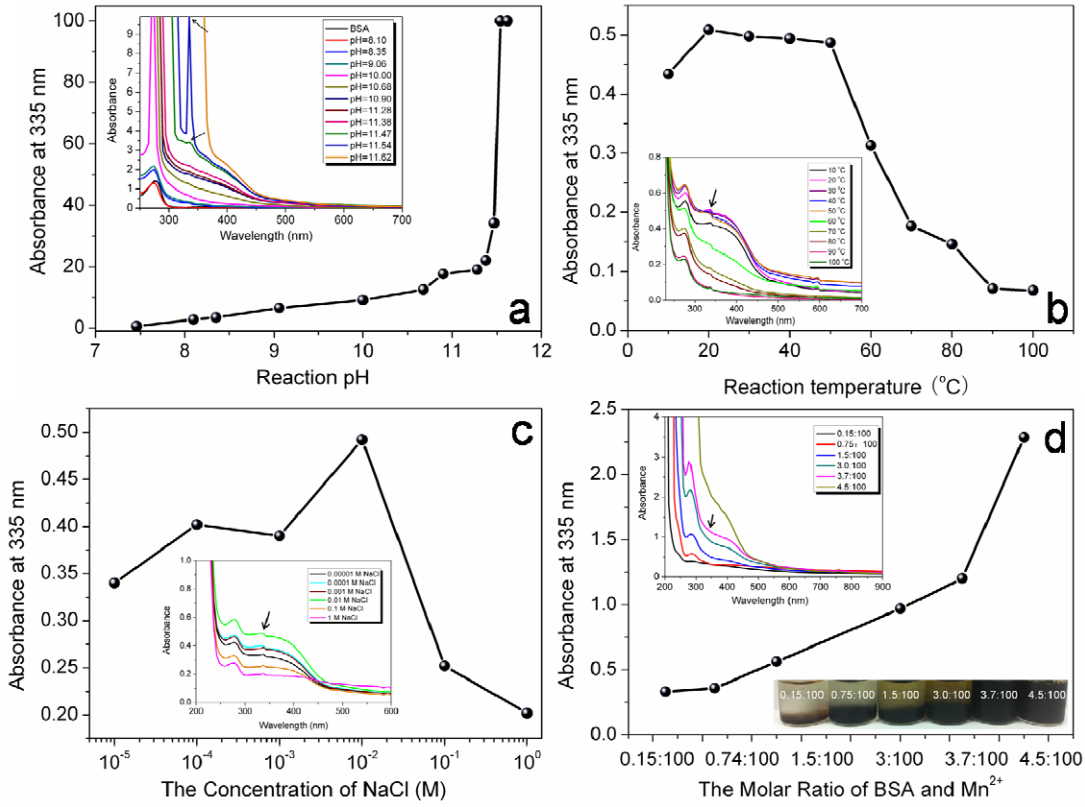

Fig. S2. Optimization of a) reaction pH from 8.10 to 11.62; b) the reaction temperature of BSA-MnO_2 NPs; c) the ionic strength of BSA-MnO_2 NPs; and d) the molar ratio of BSA and Mn^{2+} precursor. Inset: UV-vis spectra at 335 nm for MnO_2

NPs in different conditions and the styleonme of different molar ratio of BSA and Mn^{2+} precursor.

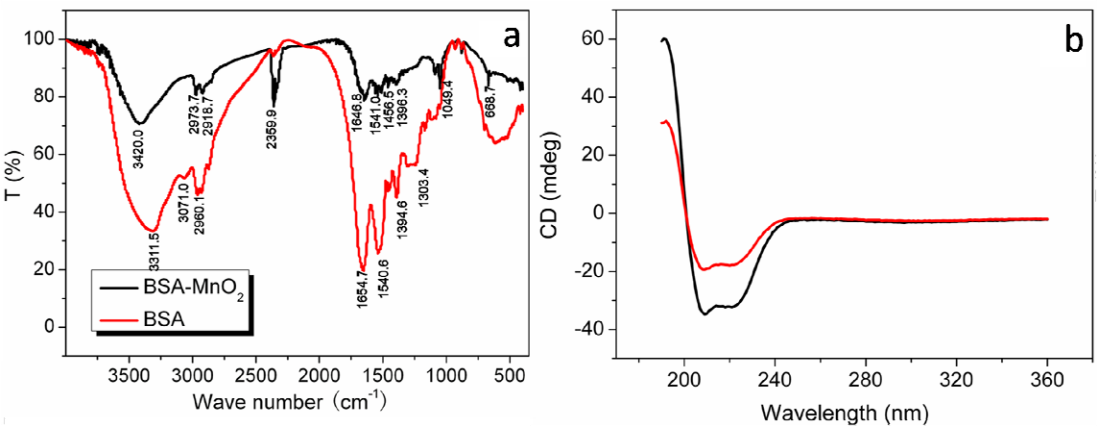

Fig. S3. a) FTIR spectra of BSA-MnO_2 NPs (black line) and pure BSA (red line); and b) CD spectra of BSA-MnO_2 NPs (red line) and pure BSA (black line).

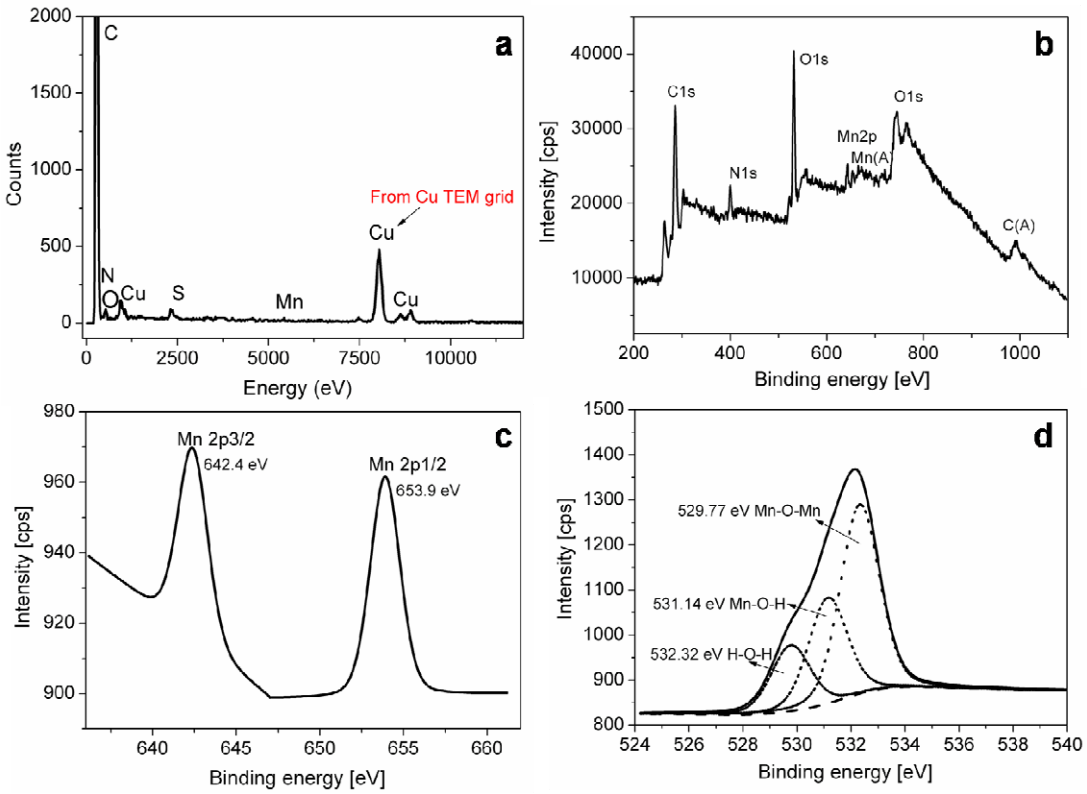

Fig. S4. a) EDX spectra of BSA-MnO_2 NPs; XPS spectra of b) BSA-MnO_2 NPs; c) Mn 2p; and d) O 1s.

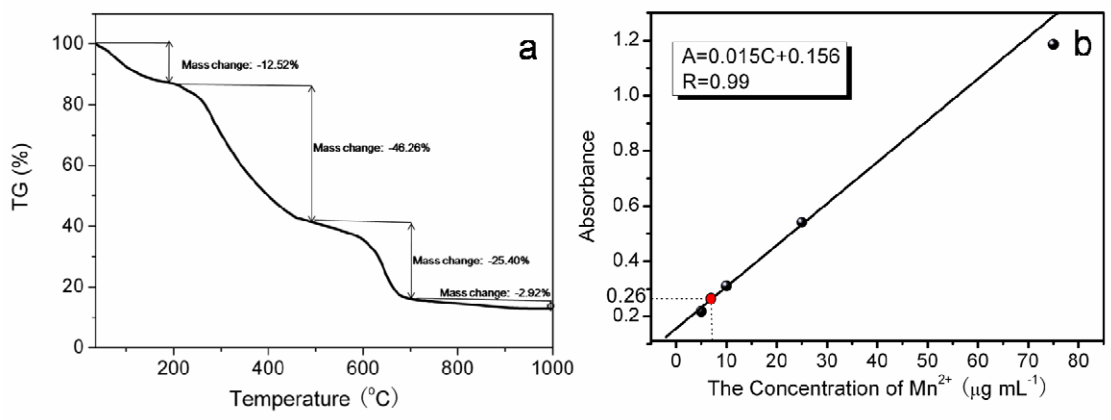

Fig. S5. a) TG of BSA-MnO_2 NPs; and b) the concentration of Mn element in BSA-MnO_2 NPs diluted 10 times by FAAS detection.

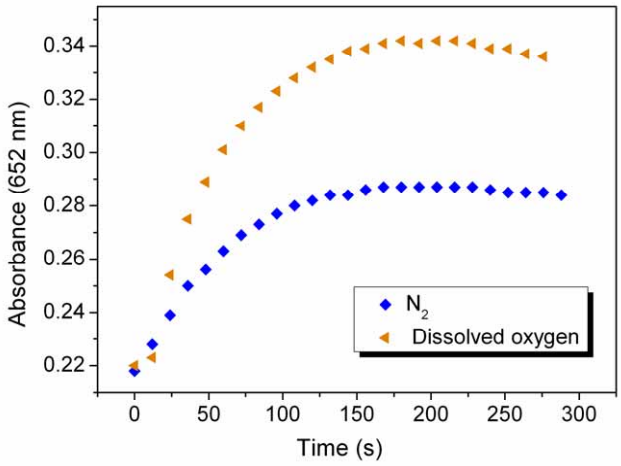

Fig. S6. Effect of dissolved oxygen (yellow line) on TMB oxidation at 35 °C and pH 4.0. The reaction rate after bubbling with high purity nitrogen for 30 minutes is greatly reduced (blue line).

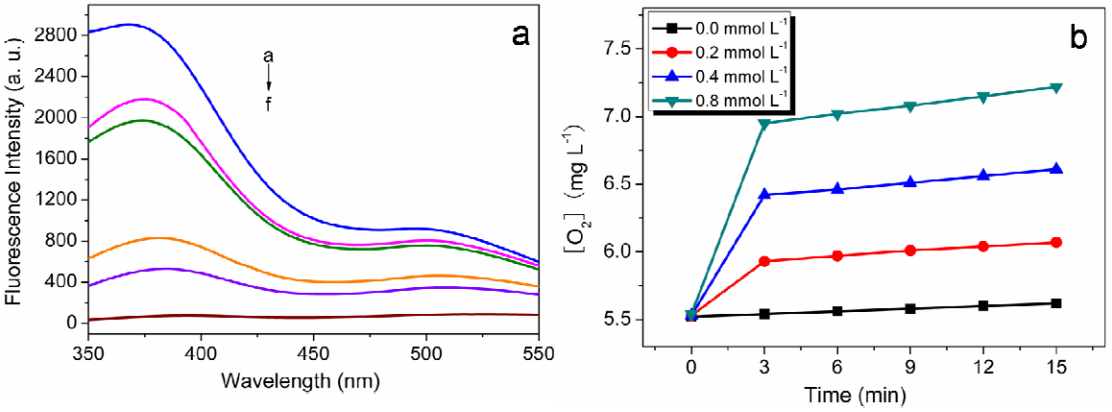

Fig. S7. a) The effect of the BSA-MnO_2 NPs on the formation of hydroxyl radical with terephthalic acid as a fluorescence probe. a-f: 7.3, 11.0, 14.0, 22.0, 27.5, 55.0 μg mL^{-1}. 10 mM H_2O_2, 0.5 mM terephthalic acid and different concentrations of the BSA-MnO_2 NPs were first incubated in 100 mM NaAc buffer (pH 5.0) exposed to UV light at 365 nm for 20 min; and b) the effect of the BSA-MnO_2 NPs concentration on the generation of O_2 by decomposition of H_2O_2. Reaction conditions: 50 mM H_2O_2 and different concentrations of BSA-MnO_2 NPs in 100 mM NaAc buffer (pH 5.0).

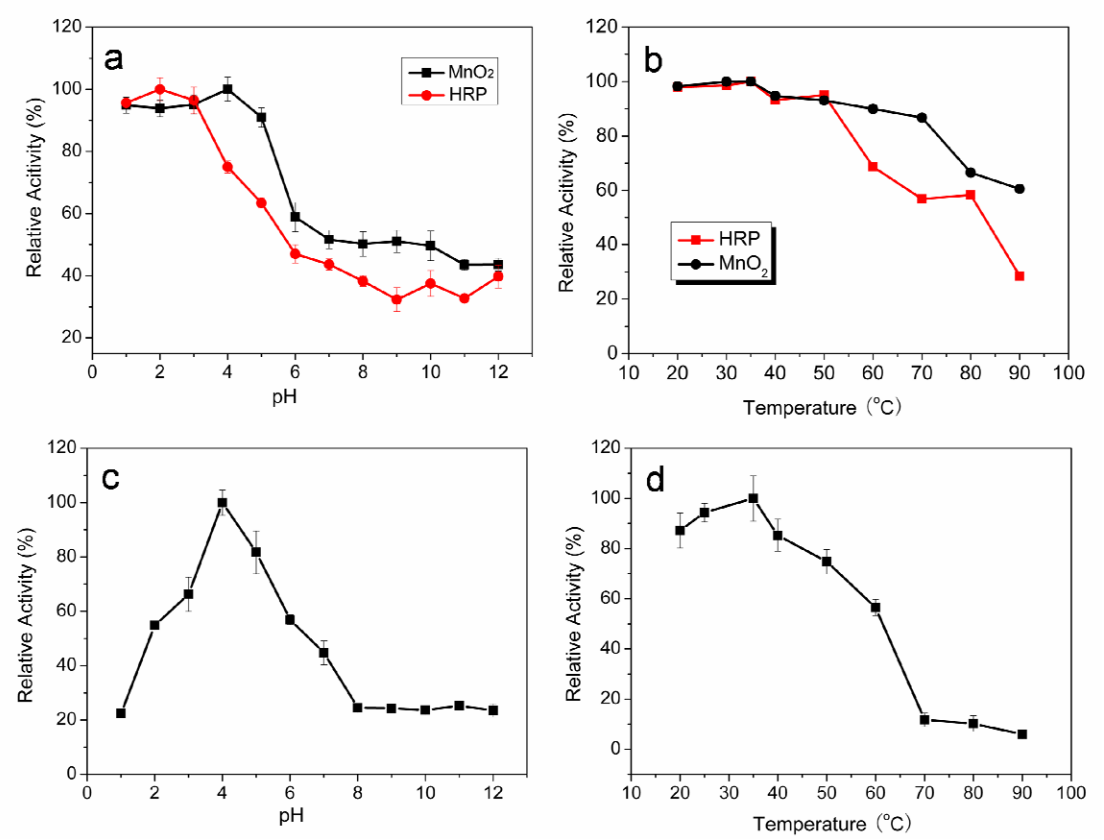

Fig. S8. Dependency of the peroxidase-like activity of BSA-MnO_2 NPs and HRP on pH a) of OPD oxidation and temperature b) of OPD oxidation with H_2O_2; and oxidase-like activity of BSA-MnO_2 NPs on pH c) of TMB oxidation and temperature d) of TMB oxidation. Experiments were carried out using 3.7 μg mL^{-1} BSA-MnO_2 NPs or 3.3 μg mL^{-1} HRP in 300 μL NaAc buffer contains 3.3 mM OPD substrate, and 3.7 μg mL^{-1} BSA-MnO_2 NPs in 300 μL citrate buffer contains 1.7 mM TMB substrate. The H_2O_2 concentration was 0.3 mM at pH 4.0 and temperature 35 °C unless otherwise stated. The maximum point in each curve was set as 100%.

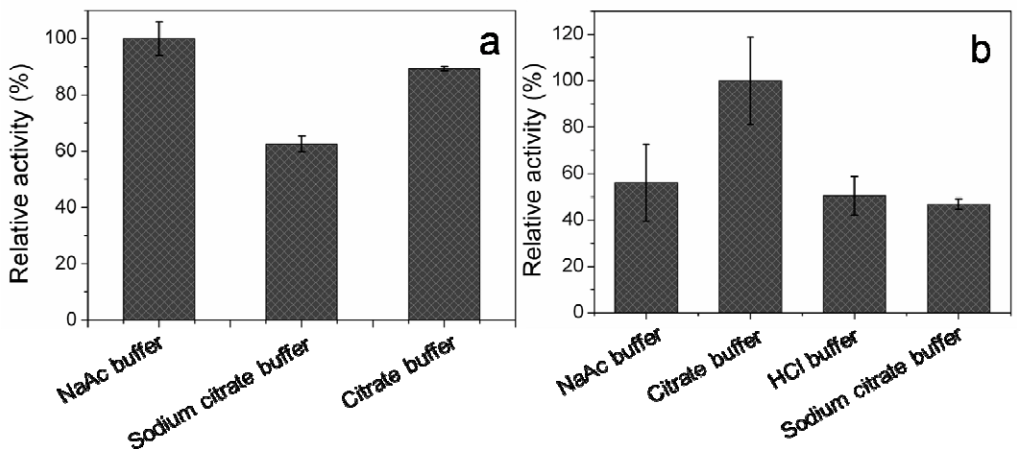

Fig. S9. Optimization conditions of all kinds of buffers a) for OPD and b) for TMB under standard conditions. 0.2 mol L^{-1} NaAc buffer (8.204 g NaAc in 500 mL deionized water using HAc adjusting pH 4.0); 0.2 mol L^{-1} citrate buffer (7.300 g $Na_2HPO_4 \cdot 2H_2O$ and 4.665 g citrate acid in 500 mL deionized water); 0.2 mol L^{-1} sodium citrate buffer (6.885 g sodium citrate in 500 mL deionized water using citrate acid adjusting pH 4.0); and HCl buffer (7.300 g $Na_2HPO_4 \cdot 2H_2O$ in 500 mL deionized water using HCl adjusting pH 4.0).

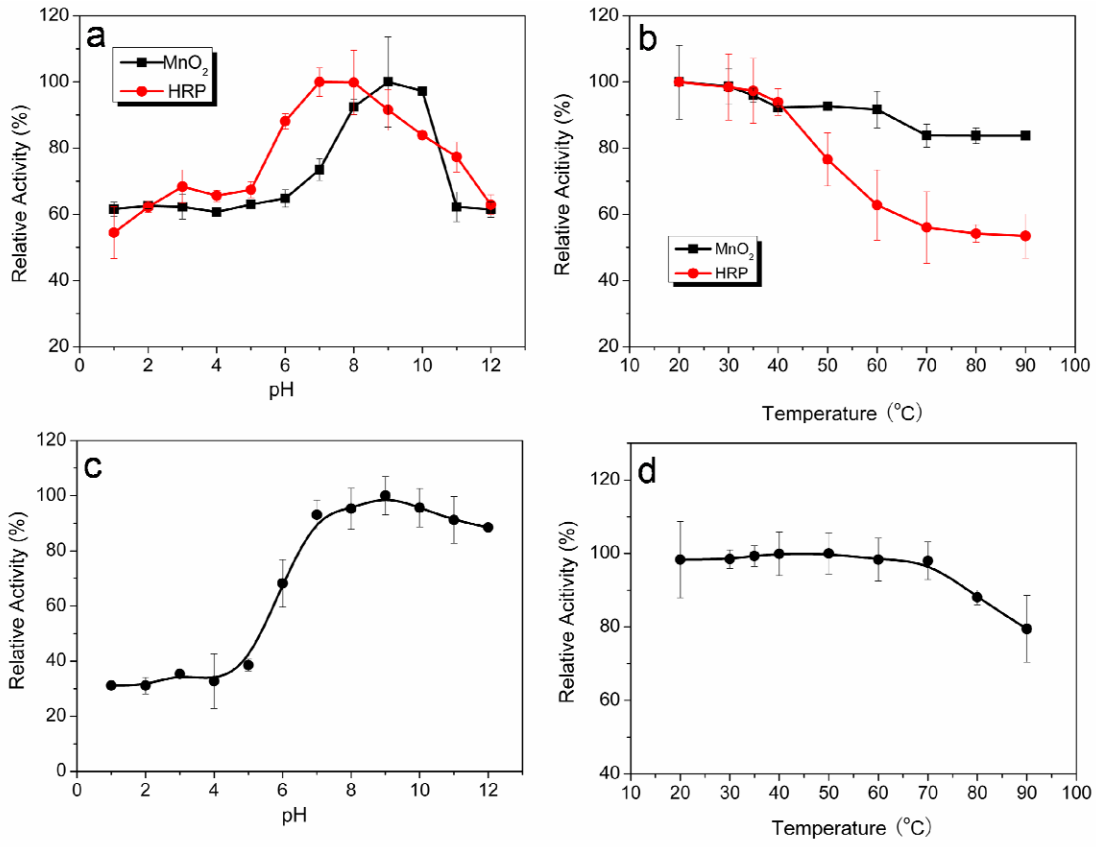

Fig. S10. a, b) The stability of BSA-MnO_2 NPs and HRP with OPD oxidation; and c, d) the stability of BSA-MnO_2 NPs with TMB oxidation. a, c) BSA-MnO_2 NPs and HRP were first incubated at pH from 1.0 to 12.0 for 2 h and then their peroxidase- and oxidase-like activities were measured; b, d) BSA-MnO_2 NPs and HRP were first incubated at temperature from 20 to 90 °C for 2 h and then the peroxidase- and oxidase-like activities were measured under standard conditions.

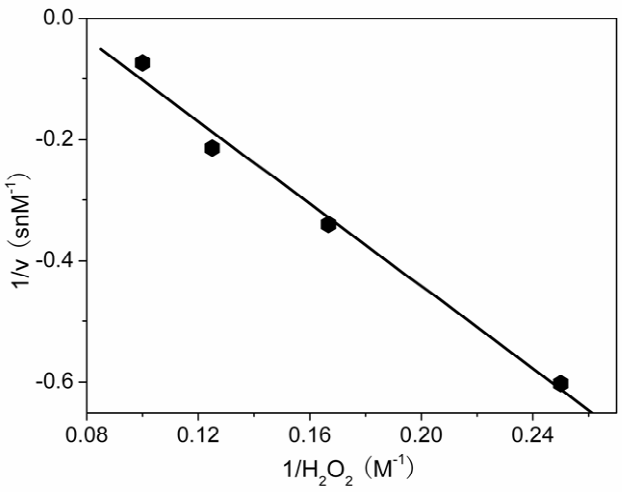

Fig. S11. Steady state kinetic assays with 3.7 μg mL^{-1} BSA-MnO_2 NPs. Double reciprocal plots of catalase activity of BSA-MnO_2 NPs and H_2O_2.

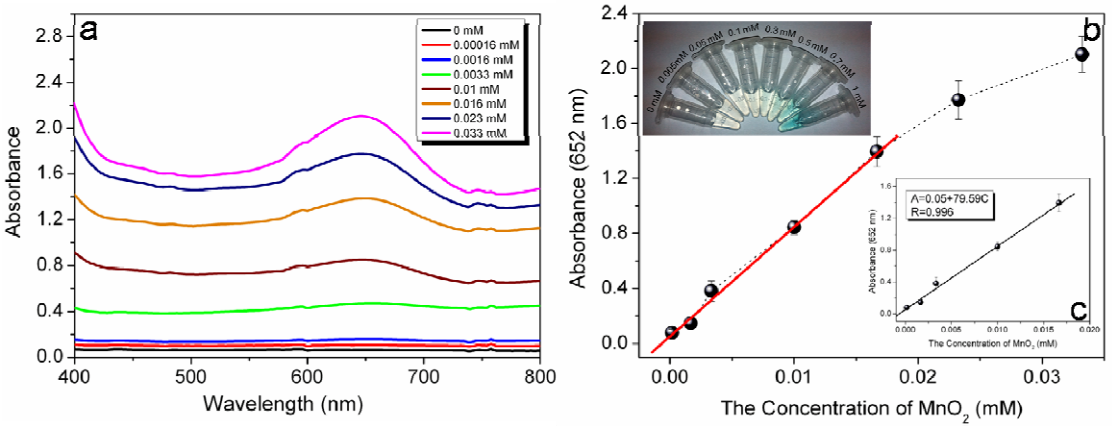

Fig. S12. a) UV-vis spectra for a solution of TMB-MnO_2 NPs in citrate buffer. The BSA-MnO_2 NPs concentrations were 0.00016, 0.0016, 0.0033, 0.010, 0.016, 0.023, 0.033 mM, respectively under standard conditions; and b) a dose-response curve for BSA-MnO_2 NPs detection. Inset: c) a linear calibration plot for detection of BSA-MnO_2 NPs.

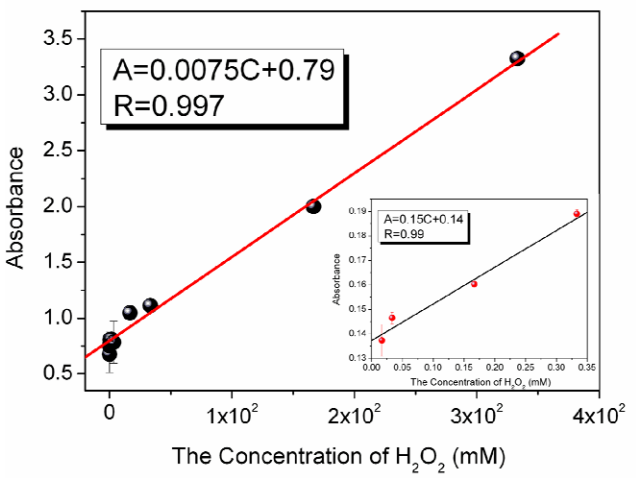

Fig. S13. A linear calibration plot for H_2O_2 detection using BSA-MnO_2 NPs as an artificial enzyme under standard conditions. Inset: a linear calibration plot for H_2O_2 using HRP as a comparison.